Contemporary Mathematics
https://ojs.wiserpub.com/index.php/CM/

Research Article

Spectral Bernoulli-Gauss Collocation Scheme for Pantograph-Type Volterra Integro-Differential Equations

R. M. Hafez[1], M. A. Abdelkawy[1], Y. H. Youssri[2], A. Biswas[3,4,5*]

[1] Department of Mathematics and Statistics, College of Science, Imam Mohammad Ibn Saud Islamic University, Riyadh, Saudi Arabia
[2] Department of Mathematics, Faculty of Science, Cairo University, Giza, 12613, Egypt
[3] Department of Mathematics & Physics, Grambling State University, Grambling, LA, 71245-2715, USA
[4] Department of Physics and Electronics, Khazar University, Baku, AZ-1096, Azerbaijan
[5] Department of Mathematics and Applied Mathematics, Sefako Makgatho Health Sciences University, Pretoria, 0204, South Africa
E-mail: biswasa@gram.edu

Received: 15 October 2025; **Revised:** 17 November 2025; **Accepted:** 25 November 2025

Abstract: In this work, we employ a spectral collocation approach to numerically solve pantograph-type Volterra integro-differential equations subject to given initial conditions. The scheme combines Bernoulli polynomials with Gauss quadrature for numerical integration. By leveraging this Bernoulli-Gauss framework, the original integro-differential problem is transformed into a solvable system of algebraic equations. Accurate approximations are achieved using only a modest number of collocation points. The convergence behavior of the method is illustrated through graphical analysis, revealing an exponential rate of convergence. To validate the proposed technique, we present several test problems whose numerical solutions are compared against exact results and those reported by alternative methods. These comparisons are summarized in tables and figures to highlight the accuracy and efficiency of the approach.

***Keywords*:** pantograph-type Volterra integro-differential equations, collocation method, Bernoulli-Gauss quadrature, Bernoulli polynomial

MSC: 45J05, 65N35, 11B68

1. Introduction

In recent years, Integro-Differential Equations (IDEs) have attracted considerable attention due to their pivotal role in modeling a wide range of phenomena across scientific and engineering disciplines [1–6]. A notable subclass of functional differential equations involves proportional delays and is commonly referred to as pantograph equations—or, more generally, generalized pantograph equations. The term "pantograph" traces back to the seminal work of Ockendon and Tayler [5], inspired by the dynamics of current collection devices on electric trains. These equations find applications in diverse areas including number theory, economics, population dynamics, control theory, electrodynamics, nonlinear dynamical systems, quantum mechanics, probability, astrophysics, cell growth models, and various industrial processes; see, for instance, [5, 7, 8] for specific examples. Both analytical properties and numerical treatments of such equations have been extensively investigated [9–12].

DOI: https://doi.org/10.37256/cm.7220268911

As a type of delay differential equation, the pantograph equation has been studied by numerous researchers from both analytical and computational perspectives. Sezer et al. [10] employed Taylor polynomials to construct approximate solutions for nonhomogeneous multi-pantograph equations. This approach was later extended in [13] to handle variable coefficients. Li and Liu [14] established sufficient conditions for the asymptotic stability of variable-step Runge-Kutta methods applied to multi-pantograph equations. Alomari et al. [15] applied the homotopy analysis method to a class of delay differential equations, while Yu and Saadatmandi [16, 17] developed a variational iteration scheme for both multi-pantograph and generalized pantograph equations. Spectral-type approximations have also been explored: Yüzbaşi [18] used Bessel polynomials, and Yalınbaş [19] employed Hermite polynomials to solve generalized pantograph equations with variable coefficients. Most recently, Tohidi et al. [20] introduced a Bernoulli collocation method based on the operational matrix of derivatives for similar problems. Recent advances in Kantorovich-type approximation operators—such as Bernstein-Kantorovich, q-Baskakov, and Sz'asz-Mirakjan variants—provide powerful tools for handling integral and delayed terms in functional equations [21–23].

In this manuscript, we develop a spectral Bernoulli-Gauss Collocation (B-GC) method for the numerical solution of m-th order pantograph-type Volterra Functional Integro-Differential Equations (VFIDEs) [18]:

$$\begin{aligned} u^{(m)}(x) = &\sum_{n=0}^{m-1} \alpha_n(x) u^{(n)}(x) + \sum_{n=0}^{m-1} \beta_n(x) u^{(n)}(p_n x + q_n) + \sum_{n=0}^{m-1} \int_0^x \kappa_{0n}(x,t) u^{(n)}(t)\, dt \\ &+ \sum_{n=0}^{m-1} \int_0^{\zeta x+\eta} \kappa_{1n}(x,t) u^{(n)}(t)\, dt + g(x), \quad x, t \in (0,\infty), \ (m \geq 1), \end{aligned} \tag{1}$$

subject to mixed initial conditions

$$\sum_{n=0}^{m-1} a_{in} u^{(n)}(0) = \lambda_i, \quad i = 0, 1, \ldots, m-1, \tag{2}$$

where $u^{(0)}(x) = u(x)$ denotes the unknown solution. The coefficient functions $\alpha_n(x)$, $\beta_n(x)$, $g(x)$, and the kernel functions $\kappa_{0n}(x,t)$, $\kappa_{1n}(x,t)$ are assumed to be sufficiently smooth on a finite interval $[a,b]$ with $0 \leq a < b < \infty$. The parameters p_n, q_n, a_{in}, ζ, η, and λ_i are real constants. Moreover, for each $n = 0, 1, \ldots, m-1$, the kernels κ_{0n} and κ_{1n} admit convergent Maclaurin series expansions.

The primary objective of this work is to construct an efficient spectral approximation $u_N(x)$ for the solution of the above VFIDEs by leveraging the properties of Bernoulli polynomials. Specifically, we introduce the Bernoulli-Gauss collocation framework, wherein $(N-m+1)$ suitably chosen collocation nodes—derived from the zeros of Bernoulli-Gauss interpolants—are employed. Together with the m initial conditions, this yields a square system of $(N+1)$ algebraic equations, which can be solved directly. As expected for spectral methods, the numerical results exhibit exponential convergence as the number of basis functions increases.

The remainder of this paper is structured as follows. Section 2 reviews the definition and essential properties of Bernoulli polynomials required for the subsequent analysis. In Section 3, we detail the construction of the Bernoulli-Gauss collocation scheme for the class of VFIDEs under consideration. Section 4 discusses the theoretical and practical accuracy of the proposed approximation. Numerical experiments demonstrating the method's efficiency and convergence behavior are presented in Section 6. Finally, concluding remarks are provided in Section 7.

2. Definition and properties of Bernoulli polynomials

It is a classical result that the Bernoulli polynomials arise from the generating function

$$\frac{\xi\, e^{\tau\xi}}{e^{\xi}-1} = e^{B(\tau)\,\xi} = \sum_{k=0}^{\infty} B_k(\tau)\frac{\xi^k}{k!}, \tag{3}$$

where, by convention, the symbolic expression $B^k(\tau)$ is interpreted as the polynomial $B_k(\tau)$. In the particular case $\xi = 0$, the values $B_k(0) = B_k$ correspond to the classical k-th Bernoulli numbers. From the generating relation (2), one deduces the well-known identities (see, e.g., [24–31])

$$B_0 = 1, \qquad (B+1)^k - B^k = B_k(1) - B_k = \delta_{1,\,k}, \tag{4}$$

where $\delta_{m,\,n}$ denotes the Kronecker delta.

Moreover, expanding the generating function yields the explicit representation (cf. [32])

$$B_k(\tau) = \sum_{\ell=0}^{k} \binom{k}{\ell} B_{k-\ell}\,\tau^{\ell}. \tag{5}$$

An equivalent recursive characterization of the Bernoulli basis polynomials $B_k(\tau)$ of degree k is given by [33]

$$\sum_{\ell=0}^{k} \binom{k+1}{\ell} B_{\ell}(\tau) = (k+1)\tau^k, \qquad k = 0,\, 1,\, \ldots. \tag{6}$$

The first several Bernoulli polynomials are

$$B_0(\tau) = 1, \quad B_1(\tau) = \tau - \tfrac{1}{2}, \quad B_2(\tau) = \tau^2 - \tau + \tfrac{1}{6}, \quad B_3(\tau) = \tau^3 - \tfrac{3}{2}\tau^2 + \tfrac{1}{2}\tau, \ \ldots$$

Furthermore, their derivatives satisfy

$$D^q B_i(\tau) = \frac{i!}{(i-q)!}\, B_{i-q}(\tau), \tag{7}$$

and, in particular,

$$D^q B_i(0) = \frac{i!}{(i-q)!}\, B_{i-q}. \tag{8}$$

These polynomials also obey the orthogonality-type relation established in [34]:

$$\int_0^1 B_i(\tau)B_j(\tau)\,d\tau = (-1)^{i-1}\frac{j!\,i!}{(j+i)!}B_{j+i}, \qquad i,\, j \geq 1. \tag{9}$$

As shown in [34], the set $\{B_k(\tau)\}_{k=0}^{\infty}$ constitutes a complete basis on the unit interval $[0,\, 1]$.

To adapt this basis to a general interval $[0,\, L]$, we introduce the shifted Bernoulli polynomials, denoted $B_k^L(\xi)$, obtained by the linear change of variable $\tau = \xi/L$ in the standard polynomials. Substituting this scaling into (5) yields the explicit form

$$B_k^L(\xi) = \sum_{\ell=0}^{k}\binom{k}{\ell}B_{k-\ell}\,\frac{\xi^\ell}{L^\ell}. \tag{10}$$

Consequently, the first few shifted polynomials on $[0,\, L]$ read

$$B_0^L(\xi) = 1, \quad B_1^L(\xi) = \frac{\xi}{L} - \frac{1}{2}, \quad B_2^L(\xi) = \frac{\xi^2}{L^2} - \frac{\xi}{L} + \frac{1}{6}, \quad B_3^L(\xi) = \frac{\xi^3}{L^3} - \frac{3}{2}\frac{\xi^2}{L^2} + \frac{1}{2}\frac{\xi}{L}, \ \ldots$$

Their derivatives follow the scaled rule

$$D^q B_i^L(\xi) = \frac{i!}{(i-q)!\,L^q}\,B_{i-q}(\xi), \tag{11}$$

and, evaluated at the origin,

$$D^q B_i^L(0) = \frac{i!}{(i-q)!\,L^q}\,B_{i-q}. \tag{12}$$

Theorem 1 The shifted Bernoulli polynomials on $[0,\, L]$ satisfy the integral identity

$$\int_0^L B_i^L(\xi)B_j^L(\xi)\,d\xi = (-1)^{i-1}\frac{j!\,i!\,L}{(j+i)!}B_{j+i}, \qquad i,\, j \geq 1.$$

Proof. Apply the substitution $\tau = \xi/L$ to the relation (9). Then

$$\int_0^1 B_i(\tau)B_j(\tau)\,d\tau = \int_0^L B_i\left(\frac{\xi}{L}\right)B_j\left(\frac{\xi}{L}\right)\frac{1}{L}\,d\xi = \frac{1}{L}\int_0^L B_i^L(\xi)B_j^L(\xi)\,d\xi$$

$$= (-1)^{i-1}\frac{j!\,i!}{(j+i)!}B_{j+i},$$

which immediately implies

$$\int_0^L B_i^L(\xi)B_j^L(\xi)\,d\xi = (-1)^{i-1}\frac{j!\,i!\,L}{(j+i)!}B_{j+i}, \qquad i,\, j \geq 1.$$

Thus, the claim is established. □

3. Bernoulli-Gauss collocation method

In this section, we apply the Bernoulli-Gauss collocation framework to obtain a numerical solution of the m-th order pantograph-type Volterra Functional Integro-Differential Equations (VFIDEs) of the form

$$\begin{aligned} u^{(m)}(\xi) &= \sum_{n=0}^{m-1}\alpha_n(\xi)u^{(n)}(\xi) + \sum_{n=0}^{m-1}\beta_n(\xi)u^{(n)}(p_n\xi+q_n) + \sum_{n=0}^{m-1}\int_0^{\xi}\kappa_{0n}(\xi,\,\tau)u^{(n)}(\tau)\,d\tau \\ &+ \sum_{n=0}^{m-1}\int_0^{\zeta\xi+\eta}\kappa_{1n}(\xi,\,\tau)u^{(n)}(\tau)\,d\tau + g(\xi), \quad \xi,\,\tau\in(0,\,L),\ (m\geq 1), \end{aligned} \tag{13}$$

subject to the initial constraints

$$\sum_{n=0}^{m-1}a_{in}u^{(n)}(0) = \lambda_i, \quad i = 0,\,1,\,\ldots,\,m-1. \tag{14}$$

The Bernoulli-Gauss collocation approach enables us to discretize the problem directly, without introducing artificial boundary conditions or performing auxiliary variable transformations. To proceed, we first establish the necessary notation.

Define the finite-dimensional space

$$S_N(0,\,L) = \text{span}\{B_0^L(\xi),\,B_1^L(\xi),\,\ldots,\,B_N^L(\xi)\}. \tag{15}$$

Let ξ_k, for $k = 0,\,1,\,\ldots,\,N$, denote the collocation nodes defined as the zeros of the $(N+1)$-th shifted Bernoulli polynomial $B_{N+1}^L(\xi)$, or alternatively, as the Gauss–Bernoulli points—i.e., the roots of $B_{N+1}^L(\xi)$ mapped to the interval $[0,\,L]$. These points generalize the role of Gauss-Legendre or Gauss-Chebyshev nodes in classical spectral methods and ensure high accuracy for polynomial interpolation and quadrature when using the shifted Bernoulli basis.

The core idea of the Bernoulli-Gauss collocation method for (13)–(14) is to seek an approximate solution $u_N(\xi) \in S_N(0,\,L)$ satisfying

$$\begin{aligned} u_N^{(m)}(\xi_k) &= \sum_{n=0}^{m-1}\alpha_n(\xi_k)u_N^{(n)}(\xi_k) + \sum_{n=0}^{m-1}\beta_n(\xi_k)u_N^{(n)}(p_n\xi_k+q_n) \\ &+ \sum_{n=0}^{m-1}\int_0^{\xi_k}\kappa_{0n}(\xi_k,\,\tau)u_N^{(n)}(\tau)\,d\tau + \sum_{n=0}^{m-1}\int_0^{\zeta\xi_k+\eta}\kappa_{1n}(\xi_k,\,\tau)u_N^{(n)}(\tau)\,d\tau \end{aligned}$$

$$+ g(\xi_k), \quad k = 0, 1, \ldots, N-m,$$

$$\sum_{n=0}^{m-1} a_{in} u_N^{(n)}(0) = \lambda_i, \quad i = 0, 1, \ldots, m-1. \tag{16}$$

We now formulate the computational algorithm. Assume the approximate solution admits the expansion

$$u_N(\xi) = \sum_{h=0}^{N} a_h B_h^L(\xi). \tag{17}$$

Using the derivative property (11), the n-th and m-th derivatives of u_N are expressed as

$$u_N^{(n)}(\xi) = \sum_{h=0}^{N} a_h D^{(n)} B_h^L(\xi) = \sum_{h=n}^{N} a_h \frac{h!}{(h-n)!L^n} B_{h-n}(\xi/L),$$

and similarly for $u_N^{(m)}(\xi)$. Substituting these representations into (13) yields

$$\begin{aligned} \sum_{h=0}^{N} a_h D^{(m)} B_h^L(\xi) = \sum_{n=0}^{m-1} \sum_{h=0}^{N} a_h \alpha_n(\xi) D^{(n)} B_h^L(\xi) + \sum_{n=0}^{m-1} \sum_{h=0}^{N} a_h \beta_n(\xi) D^{(n)} B_h^L(p_n \xi + q_n) \\ + \sum_{n=0}^{m-1} \int_0^{\xi} \kappa_{0n}(\xi, \tau) \sum_{h=0}^{N} a_h D^{(n)} B_h^L(\tau)\, d\tau \\ + \sum_{n=0}^{m-1} \int_0^{\zeta\xi+\eta} \kappa_{1n}(\xi, \tau) \sum_{h=0}^{N} a_h D^{(n)} B_h^L(\tau)\, d\tau + g(\xi). \end{aligned} \tag{18}$$

Invoking the derivative formula (11), namely $D^{(q)} B_h^L(\xi) = \frac{h!}{(h-q)!L^q} B_{h-q}(\xi/L)$, we rewrite (18) as

$$\begin{aligned} \sum_{h=m}^{N} a_h \frac{h!}{(h-m)!L^m} B_{h-m}\left(\frac{\xi}{L}\right) = \sum_{n=0}^{m-1} \sum_{h=n}^{N} a_h \frac{h!}{(h-n)!L^n} \alpha_n(\xi) B_{h-n}\left(\frac{\xi}{L}\right) \\ + \sum_{n=0}^{m-1} \sum_{h=n}^{N} a_h \frac{h!}{(h-n)!L^n} \beta_n(\xi) B_{h-n}\left(\frac{p_n \xi + q_n}{L}\right) \\ + \sum_{n=0}^{m-1} \int_0^{\xi} \kappa_{0n}(\xi, \tau) \sum_{h=n}^{N} a_h \frac{h!}{(h-n)!L^n} B_{h-n}\left(\frac{\tau}{L}\right) d\tau \end{aligned}$$

$$+\sum_{n=0}^{m-1}\int_0^{\zeta\xi+\eta}\kappa_{1n}(\xi,\,\tau)\sum_{h=n}^{N}a_h\frac{h!}{(h-n)!L^n}B_{h-n}\left(\frac{\tau}{L}\right)d\tau+g(\xi). \tag{19}$$

Similarly, inserting (17) into the initial conditions (14) and applying (12) gives

$$\sum_{n=0}^{m-1}\sum_{h=n}^{N}a_{in}a_h\frac{h!}{(h-n)!L^n}B_{h-n}=\lambda_i,\quad i=0,\,1,\,\ldots,\,m-1. \tag{20}$$

Next, we enforce equation (19) at the $(N-m+1)$ Bernoulli-Gauss collocation points ξ_k, $k=0,\,1,\,\ldots,\,N-m$, resulting in

$$\begin{aligned}\sum_{h=m}^{N}a_h\frac{h!}{(h-m)!L^m}B_{h-m}\left(\frac{\xi_k}{L}\right)&=\sum_{n=0}^{m-1}\sum_{h=n}^{N}a_h\frac{h!}{(h-n)!L^n}\alpha_n(\xi_k)B_{h-n}\left(\frac{\xi_k}{L}\right)\\&+\sum_{n=0}^{m-1}\sum_{h=n}^{N}a_h\frac{h!}{(h-n)!L^n}\beta_n(\xi_k)B_{h-n}\left(\frac{p_n\xi_k+q_n}{L}\right)\\&+\sum_{n=0}^{m-1}\int_0^{\xi_k}\kappa_{0n}(\xi_k,\,\tau)\sum_{h=n}^{N}a_h\frac{h!}{(h-n)!L^n}B_{h-n}\left(\frac{\tau}{L}\right)d\tau\\&+\sum_{n=0}^{m-1}\int_0^{\zeta\xi_k+\eta}\kappa_{1n}(\xi_k,\,\tau)\sum_{h=n}^{N}a_h\frac{h!}{(h-n)!L^n}B_{h-n}\left(\frac{\tau}{L}\right)d\tau+g(\xi_k).\end{aligned} \tag{21}$$

Finally, combining the collocation equations (21) with the initial condition constraints (22) (the simplified form of (20)),

$$\sum_{n=0}^{m-1}\sum_{h=n}^{N}a_{in}a_h\frac{h!}{(h-n)!L^n}B_{h-n}=\lambda_i, \tag{22}$$

produces a square system of $(N+1)$ algebraic equations for the unknown coefficients a_j, $j=0,\,1,\,\ldots,\,N$, which can be solved using any standard linear or nonlinear solver, depending on the nature of the problem.

4. Accuracy of the solution

The fidelity of the computed approximation can be assessed by evaluating the residual of the governing equation. Since $u_N(\xi)$ is an approximate solution of (13), substitution of u_N and its derivatives into the left-hand side of (13) should yield a quantity close to zero. Specifically, for each collocation point $\xi_q\in[0,\,L]$, $q=0,\,1,\,\ldots,\,Q-1$, we define the pointwise residual

$$E(\xi_q) = \Bigg| u_N^{(m)}(\xi_q) - \sum_{n=0}^{m-1} \alpha_n(\xi_q) u_N^{(n)}(\xi_q) - \sum_{n=0}^{m-1} \beta_n(\xi_q) u_N^{(n)}(p_n \xi_q + q_n)$$

$$- \sum_{n=0}^{m-1} \int_0^{\xi_q} \kappa_{0n}(\xi_q, \tau) u_N^{(n)}(\tau)\, d\tau - \sum_{n=0}^{m-1} \int_0^{\zeta \xi_q + \eta} \kappa_{1n}(\xi_q, \tau) u_N^{(n)}(\tau)\, d\tau - g(\xi_q) \Bigg|.$$

In practice, the collocation points $\{\xi_q\}_{q=0}^{Q-1}$ are typically selected as the Gauss-Lobatto or Chebyshev-Gauss-Lobatto nodes associated with the spectral basis used to construct u_N; this choice ensures good resolution across the domain and compatibility with the approximation space. Derivatives $u_N^{(n)}$ are evaluated efficiently via spectral differentiation matrices or recurrence relations intrinsic to the chosen basis (e.g., Chebyshev or Legendre polynomials). The Volterra-type integrals are computed using high-order quadrature rules—such as Gauss-Legendre or Clenshaw-Curtis quadrature—applied on subintervals aligned with the collocation grid. Delayed arguments $p_n \xi_q + q_n$ are handled by evaluating $u_N^{(n)}$ at off-grid points via polynomial interpolation or barycentric formulas, preserving spectral accuracy.

The residual $E(\xi_q)$ is then monitored during the solution process. For each trial value of the truncation index N, we compute $\max_q E(\xi_q)$. If a uniform accuracy level 10^{-r} is desired, N is incrementally increased until the condition

$$\max_{0 \le q < Q} E(\xi_q) < 10^{-r}$$

is satisfied. This adaptive strategy ensures that the approximation meets the prescribed tolerance while avoiding unnecessary computational cost. Similar residual-based stopping criteria have been employed in spectral collocation methods for functional differential and integro-differential equations; see, e.g., [35–41].

Alternatively, the global residual function is defined as

$$E_N(\xi) = u_N^{(m)}(\xi) - \sum_{n=0}^{m-1} \alpha_n(\xi) u_N^{(n)}(\xi) - \sum_{n=0}^{m-1} \beta_n(\xi) u_N^{(n)}(p_n \xi + q_n)$$

$$- \sum_{n=0}^{m-1} \int_0^{\xi} \kappa_{0n}(\xi, \tau) u_N^{(n)}(\tau)\, d\tau - \sum_{n=0}^{m-1} \int_0^{\zeta \xi + \eta} \kappa_{1n}(\xi, \tau) u_N^{(n)}(\tau)\, d\tau - g(\xi).$$

If $E_N(\xi) \to 0$ as $N \to \infty$, the method is convergent, and the approximation error diminishes accordingly.

5. Convergence analysis and stability consideration

5.1 *Convergence analysis*

Let $H = L^2[0, L]$ denote the Hilbert space of square-integrable functions on $[0, L]$, and let

$$U = \text{span}\{B_0^L(\xi), B_1^L(\xi), \ldots, B_N^L(\xi)\}$$

be a finite-dimensional subspace of H. Since U is closed and finite-dimensional, it is complete under the L^2-norm.

Lemma 1 ([42]) For any $u(\xi) \in H$, there exists a unique best approximation $u_N(\xi) \in U$ such that

$$\|u - u_N\|_2 \leq \|u - y\|_2 \quad \text{for all } y \in U.$$

Moreover, this best approximation satisfies the orthogonality condition

$$\langle u - u_N, y \rangle = 0 \quad \text{for all } y \in U,$$

where $\langle \cdot, \cdot \rangle$ denotes the inner product in H. Consequently, $u(\xi)$ can be approximated by

$$u_N(\xi) = \sum_{k=0}^{N} a_k B_k^L(\xi).$$

Lemma 2 ([43]) Suppose $u(\xi) \in C^{N+1}[0, L]$, and let $u_N(\xi)$ be its best approximation in U. Then the error satisfies

$$\|u - u_N\|_2 \leq \frac{A}{(N+1)!} \frac{L^{N+\frac{3}{2}}}{\sqrt{2N+3}},$$

where

$$A = \max_{\xi \in [0, L]} \left| u^{(N+1)}(\xi) \right|.$$

The assumption that $u \in C^{N+1}[0, L]$ is essential for the validity of this error estimate. For pantograph-type equations—i.e., delay differential equations involving proportional delays of the form $u(p\xi)$ with $0 < p < 1$—the regularity of the solution depends critically on the smoothness of the coefficient functions, the forcing term, and the compatibility of initial conditions at the origin. Under standard hypotheses (e.g., analytic coefficients and right-hand side, together with consistent initial data), it is well known that solutions to linear pantograph equations are analytic on $[0, L]$; see, for instance, [5, 11]. Analyticity implies membership in $C^{N+1}[0, L]$ for any finite N, thereby justifying the smoothness assumption required by Lemma 2. In the nonlinear or non-smooth coefficient case, however, reduced regularity may occur, and the factorial decay in the error bound would no longer hold uniformly. In such scenarios, alternative error analyses based on Sobolev regularity or piecewise-smooth approximations may be more appropriate.

Lemma 3 If $u^{(i)}(\xi) \in C^{N+1}[0, L]$ and $u_N^{(i)}$ is the best approximation to $u^{(i)}$ in U, then

$$\|u^{(i)} - u_N^{(i)}\|_2 \leq \frac{A_i}{(N+1)!} \frac{L^{N+\frac{3}{2}}}{\sqrt{2N+3}},$$

where $A_i = \max_{\xi \in [0, L]} \left| u^{(N+i+1)}(\xi) \right|$.

Now consider the exact equation

$$g(\xi) = u^{(m)}(\xi) - \sum_{n=0}^{m-1} \Big[\alpha_n(\xi) u^{(n)}(\xi) + \beta_n(\xi) u^{(n)}(p_n\xi + q_n) + \int_0^{\xi} \kappa_{0n}(\xi, \tau) u^{(n)}(\tau)\, d\tau + \int_0^{\zeta\xi+\eta} \kappa_{1n}(\xi, \tau) u^{(n)}(\tau)\, d\tau \Big],$$

and the corresponding residual of the approximate solution:

$$|R_N(\xi)| = \Big| u_N^{(m)}(\xi) - \sum_{n=0}^{m-1} \Big[\alpha_n(\xi) u_N^{(n)}(\xi) + \beta_n(\xi) u_N^{(n)}(p_n\xi + q_n) + \int_0^{\xi} \kappa_{0n}(\xi, \tau) u_N^{(n)}(\tau)\, d\tau + \int_0^{\zeta\xi+\eta} \kappa_{1n}(\xi, \tau) u_N^{(n)}(\tau)\, d\tau \Big] - g(\xi) \Big|.$$

Applying the triangle inequality and bounding each term using uniform norms, we obtain

$$|R_N(\xi)| \le |u^{(m)}(\xi) - u_N^{(m)}(\xi)| + \sum_{n=0}^{m-1} \Big[\alpha_n^{\max} |u^{(n)}(\xi) - u_N^{(n)}(\xi)| + \beta_n^{\max} |u^{(n)}(p_n\xi + q_n) - u_N^{(n)}(p_n\xi + q_n)| + \int_0^{\xi} \kappa_{0n}^{\max} |u^{(n)}(\tau) - u_N^{(n)}(\tau)|\, d\tau + \int_0^{\zeta\xi+\eta} \kappa_{1n}^{\max} |u^{(n)}(\tau) - u_N^{(n)}(\tau)|\, d\tau \Big],$$

where we define the uniform bounds

$$\alpha = \max_{0 \le n \le m-1} \alpha_n^{\max}, \quad \alpha_n^{\max} = \max_{\xi \in [0, L]} |\alpha_n(\xi)|,$$

$$\beta = \max_{0 \le n \le m-1} \beta_n^{\max}, \quad \beta_n^{\max} = \max_{\xi \in [0, L]} |\beta_n(\xi)|,$$

$$\kappa_{0n}^{\max} = \max_{(\xi, \tau) \in [0, L]^2} |\kappa_{0n}(\xi, \tau)|, \quad \kappa_0 = \max_{0 \le n \le m-1} \kappa_{0n}^{\max},$$

$$\kappa_{1n}^{\max} = \max_{(\xi, \tau) \in [0, L]^2} |\kappa_{1n}(\xi, \tau)|, \quad \kappa_1 = \max_{0 \le n \le m-1} \kappa_{1n}^{\max}.$$

Since $\|f\|_\infty \le \|f\|_2$ for $f \in L^2[0, L]$, and using Lemma 3, we derive the global error estimate

$$|R_N(\xi)| \le \frac{A_m}{(N+1)!} \frac{L^{N+\frac{3}{2}}}{\sqrt{2N+3}} + \sum_{n=0}^{m-1} \frac{[\alpha + \beta + \kappa_0 L + \kappa_1(\zeta L + \eta)] A_n}{(N+1)!} \frac{L^{N+\frac{3}{2}}}{\sqrt{2N+3}}.$$

Thus, the residual satisfies

$$|R_N(\xi)| \leq \frac{A_m + \varepsilon \widetilde{A}_m}{(N+1)!} \frac{mL^{N+\frac{3}{2}}}{\sqrt{2N+3}},$$

where

$$\varepsilon = \alpha + \beta + \kappa_0 L + \kappa_1(\zeta L + \eta), \qquad \widetilde{A}_m = \max\{A_0, A_1, \ldots, A_{m-1}\}.$$

This bound confirms that the residual decays factorially with N, reflecting the spectral (exponential) convergence of the method.

5.2 *Stability consideration*

The convergence estimate above presumes that the discrete system resulting from collocation is well-conditioned and that small perturbations in the data (e.g., in g, α_n, β_n, or the kernels) lead to correspondingly small changes in the computed solution u_N. For the class of linear pantograph-type equations considered here, stability of the spectral collocation method is closely tied to the invertibility and boundedness of the discrete operator. Under the same regularity and compatibility assumptions that guarantee analyticity of the exact solution (e.g., smooth coefficients, non-resonant delay parameters, and consistent initial conditions), the collocation matrix is typically nonsingular for sufficiently large N, and its condition number grows at most algebraically with N—a standard feature of spectral methods for well-posed linear problems. Moreover, because the basis $\{B_k^L\}$ is chosen to be well-conditioned (e.g., orthogonal polynomials mapped to $[0, L]$), and because the collocation points are selected to avoid Runge-type instabilities (e.g., Chebyshev-Gauss-Lobatto nodes), the method exhibits numerical stability in practice. In the presence of highly oscillatory or stiff components, however, preconditioning or reformulation (e.g., via integration or variable transformation) may be necessary to maintain stability. Nonetheless, for the smooth, analytic regimes assumed throughout this analysis, the proposed scheme is both convergent and stable in the sense of continuous dependence on input data.

6. Numerical results

To demonstrate the efficacy of the B-GC method in solving pantograph-type Volterra functional integro-differential equations, we present several illustrative test problems.

Example 1 ([18]) Consider the first-order pantograph-type Volterra integro-differential equation

$$u'(\xi) = 2e^{1-\xi} - 3u(\xi) - 3\int_{\xi-1}^{\xi} u(\tau)\,d\tau - \int_{\xi-1}^{\xi} u'(\tau)\,d\tau, \tag{23}$$

subject to the initial condition $u(0) = 1$ on the interval $[0, 2]$. The exact solution is $u(\xi) = e^{-\xi}$. By splitting the integrals at the lower limit, the equation can be equivalently rewritten as

$$\begin{cases} u'(\xi) = 2e^{1-\xi} - 3u(\xi) - 3\int_0^{\xi} u(\tau)\,d\tau - \int_0^{\xi} u'(\tau)\,d\tau + 3\int_0^{\xi-1} u(\tau)\,d\tau + \int_0^{\xi-1} u'(\tau)\,d\tau, \\ u(0) = 1. \end{cases}$$

In this formulation, the parameters are identified as: $m = 1$, $\zeta = 1$, $\eta = -1$, $\alpha_0(\xi) = -3$, $\kappa_{00}(\xi, \tau) = -3$, $\kappa_{01}(\xi, \tau) = -1$, $\kappa_{10}(\xi, \tau) = 3$, $\kappa_{11}(\xi, \tau) = 1$, and $g(\xi) = 2e^{1-\xi}$.

Table 1 compares the maximum absolute errors of the B-GC method (with $N = 15$) against several spline-based collocation schemes [44]—including shifted Gauss, Radau II, Lobatto, Gauss I, and other configurations—as well as the Laguerre collocation approach [18]. The absolute errors produced by the B-GC method with $N = 22$ are displayed in Figure 1, confirming high accuracy across the domain.

Table 1. Maximum absolute errors for problem (23)

Gauss (60 collocation points) [44]	1.30×10^{-10}
Radau II (60 points) [44]	4.67×10^{-9}
Lobatto (60 points) [44]	1.13×10^{-7}
Gauss I (40 points) [44]	6.57×10^{-8}
Other (60 points) [44]	5.85×10^{-7}
Laguerre (15 points) [18]	2.93×10^{-10}
Bernoulli (15 points)	2.28×10^{-11}

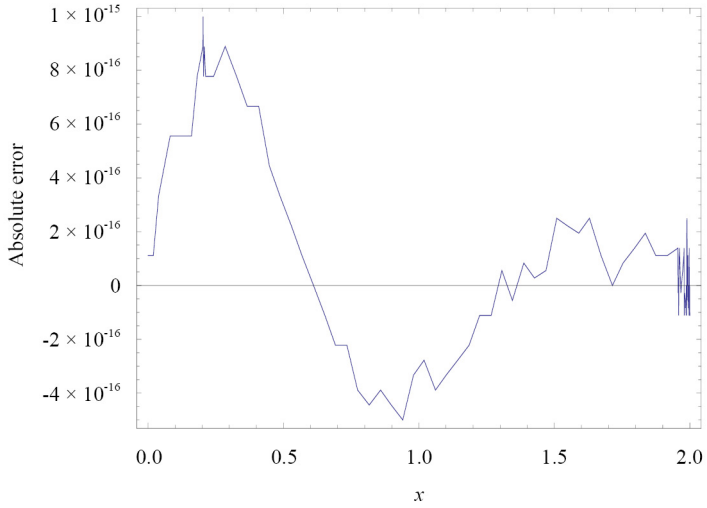

Figure 1. Absolute error distribution for $N = 22$ in Example 1

Example 2 ([18]) We now examine the first-order pantograph-type Volterra integro-differential equation

$$u'(\xi) = u(\xi - 1) + \int_{\xi}^{\xi - 1} u(\tau)\, d\tau, \tag{24}$$

with initial condition $u(0) = 1$. The exact solution is $u(\xi) = e^{\xi}$. Rewriting the integral with consistent limits yields

$$\begin{cases} u'(\xi) = u(\xi - 1) - \int_0^{\xi-1} u(\tau)\, d\tau + \int_0^{\xi} u(\tau)\, d\tau, \\ u(0) = 1. \end{cases}$$

As shown in Table 2, the B-GC method achieves machine-level precision when $N = 24$, significantly outperforming the Laguerre collocation results at $N = 8$. Figure 2 illustrates the close agreement between the exact and numerical solutions at $N = 24$.

Table 2. Absolute errors for Example 2

ξ_i	Laguerre collocation [18]	B-GC method	
		$N = 8$	$N = 24$
0.0	3.1308×10^{-14}	4.4408×10^{-16}	2.2204×10^{-16}
0.2	1.5829×10^{-6}	1.6131×10^{-6}	2.2204×10^{-16}
0.4	2.1689×10^{-6}	5.0686×10^{-7}	2.2204×10^{-16}
0.6	2.0004×10^{-6}	1.7005×10^{-6}	0
0.8	1.7385×10^{-6}	3.1650×10^{-6}	4.4408×10^{-16}
1.0	1.8455×10^{-6}	3.3140×10^{-6}	0

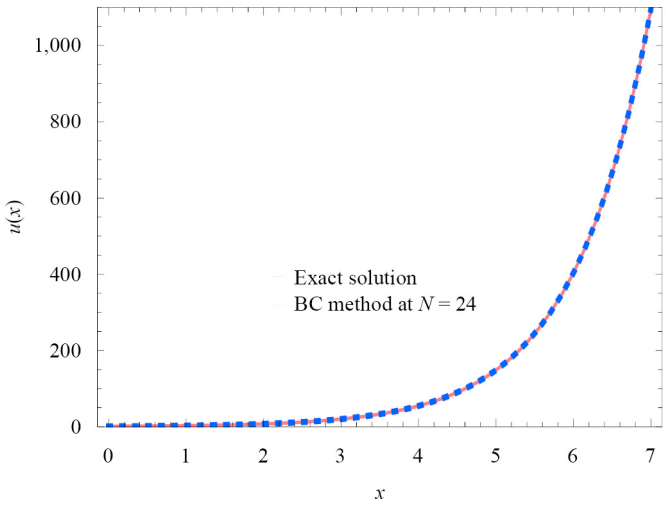

Figure 2. Exact and approximate solutions ($N = 24$) for Example 2

Example 3 ([45]) Consider the first-order pantograph-type Volterra integro-differential equation

$$\begin{aligned} u'(\xi) = {} & 3\cos(\xi) - \tfrac{1}{4}\cos(3\xi - 1) - 2 + \tfrac{1}{2}(\sin(\xi) + 1) + \sin(2\xi) - 2\cos(\xi - 1) \\ & + \tfrac{1}{4}\cos(3\xi + 1) - 2\sin(2\xi + 1) + \int_{\xi-1}^{\xi} \big(\cos(\xi + \tau + 1) + 2\big) u(\tau)\, d\tau, \end{aligned} \tag{25}$$

with $u(0) = 1$ on $[0, 3]$. The exact solution is $u(\xi) = \sin(\xi) + 1$. Reformulating the integral over $[0, \xi]$ and $[0, \xi - 1]$ gives

$$\begin{cases} u'(\xi) = 3\cos(\xi) - \frac{1}{4}\cos(3\xi - 1) - 2 + \frac{1}{2}(\sin(\xi) + 1) + \sin(2\xi) - 2\cos(\xi - 1) \\ \qquad + \frac{1}{4}\cos(3\xi + 1) - 2\sin(2\xi + 1) + \int_0^{\xi} \big(\cos(\xi + \tau + 1) + 2\big) u(\tau)\, d\tau \\ \qquad - \int_0^{\xi - 1} \big(\cos(\xi + \tau + 1) + 2\big) u(\tau)\, d\tau, \\ u(0) = 1. \end{cases}$$

Table 3. Absolute errors for Example 3

ξ_i	Taylor collocation [45]		B-GC method	
	$N = 16$	$N = 25$	$N = 16$	$N = 25$
0.5	1.04×10^{-6}	1.0×10^{-9}	6.82×10^{-13}	0
1.0	2.13×10^{-6}	7.0×10^{-9}	1.06×10^{-12}	0
1.5	3.03×10^{-6}	1.3×10^{-8}	1.51×10^{-12}	1.11×10^{-16}
2.0	4.12×10^{-6}	2.6×10^{-8}	2.38×10^{-12}	2.22×10^{-16}
2.5	6.19×10^{-6}	4.7×10^{-8}	5.19×10^{-11}	1.11×10^{-15}
3.0	1.0×10^{-5}	8.9×10^{-8}	5.31×10^{-9}	4.74×10^{-15}

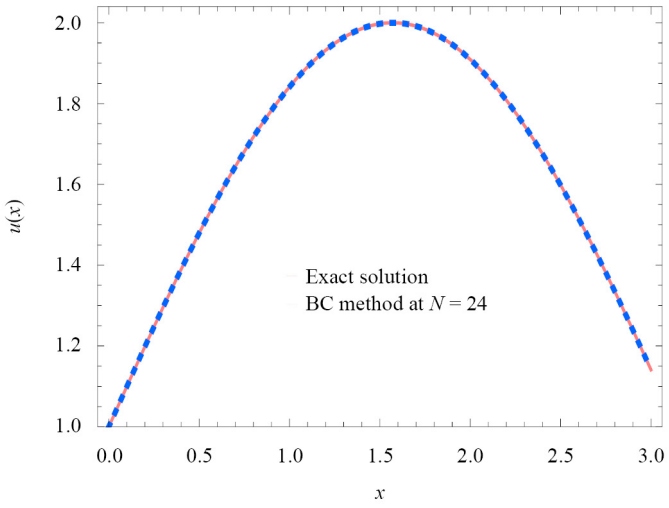

Figure 3. Exact and approximate solutions ($N = 24$) for Example 3

Table 3 demonstrates that the B-GC method consistently achieves errors several orders of magnitude smaller than the Taylor collocation approach [45], even at comparable polynomial degrees. Figure 3 visually confirms the excellent agreement between the numerical and exact solutions.

Example 4 Consider the first-order pantograph-type Volterra integro-differential equation

$$\begin{cases} u'(\xi) = \frac{6\xi^2}{\Gamma(3)} - \frac{\xi^2 e^{\xi}}{5} u(\xi) - \frac{(0.5\xi)^2}{5} u(0.5\xi) + \int_0^{\xi} e^{\xi} \tau u(\tau)\, d\tau + \int_0^{0.5\xi} \tau u(\tau)\, d\tau, \\ u(0) = 0, \end{cases}$$

whose exact solution is $u(\xi) = \xi^3$.

The results in Table 4 clearly show that the proposed B-GC method achieves significantly higher accuracy than the Euler wavelet approach at all evaluation points. The absolute errors decrease from the order of 10^{-5} for Euler wavelets to as low as 10^{-9} when using $N = 14$. Increasing N from 10 to 14 further improves the accuracy, reflecting the stability and efficiency of our method.

Moreover, the CPU times highlight a major advantage of the B-GC method: it delivers these high-accuracy results with a dramatically lower computational cost, reducing the runtime from nearly 2,000 seconds to under 4 seconds. Overall, the table demonstrates that the proposed B-GC method is both highly accurate and computationally efficient.

Table 4. Absolute errors for Example 4

ξ_i	Euler wavelets [46]	B-GC method	
		$N = 10$	$N = 14$
0.1	3.51559×10^{-5}	3.58313×10^{-8}	5.03386×10^{-9}
0.3	2.73292×10^{-5}	1.04937×10^{-7}	1.06554×10^{-8}
0.5	9.76814×10^{-5}	1.45451×10^{-7}	1.05403×10^{-8}
0.7	2.72777×10^{-5}	1.59945×10^{-7}	8.22383×10^{-9}
0.9	3.51115×10^{-5}	1.70188×10^{-7}	7.23477×10^{-9}
CPU	1994.64	2.813	3.967

Example 5 ([47]) Finally, we solve the second-order problem

$$\begin{cases} u''(\xi) - \frac{3}{4} u(\xi) + u\left(\frac{\xi}{2}\right) = -\frac{11}{4} \sin(\xi) + \sin\left(\frac{\xi}{2}\right) + \xi \cos(\xi) + \int_0^{\xi} \tau u(\tau)\, d\tau, \\ u(0) = 0, \quad u'(0) = 1, \end{cases}$$

whose exact solution is $u(\xi) = \sin(\xi)$.

Table 5 shows that while the B-GC method with $N = 10$ yields errors comparable to the Taylor method, increasing N to 20 drives the error down to machine precision. Figure 4 displays the decay of the absolute values of the expansion coefficients $|a_j|$ on a logarithmic scale, revealing rapid (exponential) decay—a hallmark of spectral convergence.

Table 5. Absolute errors for Example 5

ξ_i	Taylor collocation ($N = 10$) [47]	B-GC method	
		$N = 10$	$N = 20$
0.2	7.00×10^{-10}	2.05×10^{-9}	8.04×10^{-16}
0.4	1.50×10^{-9}	5.42×10^{-9}	7.21×10^{-16}
0.6	2.40×10^{-9}	4.75×10^{-9}	6.66×10^{-16}
0.8	3.00×10^{-9}	4.03×10^{-10}	7.77×10^{-16}
1.0	1.06×10^{-7}	3.58×10^{-9}	7.77×10^{-16}

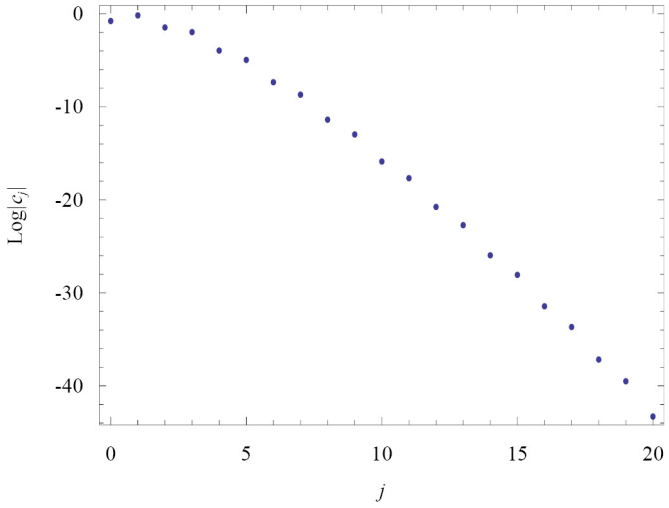

Figure 4. Logarithmic plot of absolute Bernoulli coefficients $|a_j|$ for $N = 20$ in Example 5

7. Concluding remarks

In this work, a spectral collocation framework is developed and employed for the numerical treatment of pantograph-type Volterra integro-differential equations. The method relies on shifted Bernoulli polynomials as basis functions in conjunction with Gauss quadrature for accurate evaluation of integral terms. High-precision results are achieved using only a modest number of Bernoulli-Gauss Collocation nodes. The convergence behavior of the scheme is also analyzed and discussed.

Despite its efficiency and spectral accuracy for smooth problems, the present method has certain limitations. First, it assumes sufficient regularity (indeed, analyticity) of the solution, which may not hold in the presence of discontinuous coefficients, nonsmooth forcing terms, or incompatible initial conditions—situations that can lead to reduced convergence rates or Gibbs-type oscillations near singularities. Second, the method is currently formulated for linear problems; its extension to nonlinear pantograph equations would require robust iterative solvers (e.g., Newton-Kantorovich schemes) and careful treatment of nonlinear delay and integral terms. Third, while the use of global polynomials yields exponential convergence for smooth solutions, it may become less efficient for problems with localized sharp gradients or long-time integration, where adaptive or hybrid strategies (e.g., domain decomposition or wavelet bases) could be more suitable.

Future research directions include: (i) generalizing the framework to systems of coupled pantograph equations arising in population dynamics or control theory; (ii) incorporating variable delays and non-constant scaling factors beyond the

affine form $p_n\xi + q_n$; (iii) developing error estimators for adaptive selection of collocation points and basis size; and (iv) exploring alternative bases—such as those inspired by recent Kantorovich-type operators [21–23]—to enhance robustness for weakly regular solutions.

The proposed method is broadly applicable to models involving proportional delays and memory effects, which appear in diverse fields such as electrodynamics (e.g., transmission line models), population biology (e.g., delayed birth processes), stochastic control, and viscoelasticity. Its spectral accuracy and modular structure make it particularly well-suited for problems where high fidelity and smooth solutions are expected, and where traditional step-by-step methods (e.g., Runge-Kutta) become computationally prohibitive due to the non-local nature of delays and integrals.

Acknowledgement

This work of the last author (AB) was supported by Grambling State University as the Endowed Chair of Mathematics. The author thankfully acknowledges this support.

Conflict of interest

The authors declare no competing financial interest.

References

[1] Behiry SH. Solution of nonlinear Fredholm integro-differential equations using a hybrid of block pulse functions and normalized Bernstein polynomials. *Journal of Computational and Applied Mathematics*. 2014; 260: 258-265.

[2] Berenguer MI, Garralda-Guillem AI, Galán MR. An approximation method for solving systems of Volterra integro-differential equations. *Applied Numerical Mathematics*. 2013; 67: 126-135.

[3] Kashkaria BSH, Syam MI. Evolutionary computational intelligence in solving a class of nonlinear Volterra-Fredholm integro-differential equations. *Journal of Computational and Applied Mathematics*. 2017; 311: 314-323.

[4] Pishbin S. Operational Tau method for singular system of Volterra integro-differential equations. *Journal of Computational and Applied Mathematics*. 2017; 311: 205-214.

[5] Ockendon JR. The dynamic of a current collection system for an electric locomotive. *Proceedings of the Royal Society of London Series A*. 1971; 322: 447-468.

[6] Tayler AB. *Mathematical Models in Applied Mathematics*. Oxford: Clarendon Press; 1986.

[7] Ajello WG, Freedman HI, Wu J. A model of stage structured population growth with density dependent time delay. *SIAM Journal on Applied Mathematics*. 1992; 52: 855-869.

[8] Buhmann MD, Iserles A. Stability of the discretized pantograph differential equation. *Mathematics of Computation*. 1993; 60: 575-589.

[9] Feldstein A, Liu Y. On neutral functional differential equations with variable time delays. *Mathematical Proceedings of the Cambridge Philosophical Society*. 1998; 124: 371-384.

[10] Sezer M. A method for the approximate solution of the second order linear differential equations in terms of Taylor polynomials. *International Journal of Mathematical Education in Science and Technology*. 1996; 27: 821-834.

[11] Liu MZ, Li D. Properties of analytic solution and numerical solution and multi-pantograph equation. *Applied Mathematics and Computation*. 2004; 155: 853-871.

[12] Shakeri F, Dehghan M. Solution of the delay differential equations via homotopy perturbation method. *Mathematics and Computational Modelling*. 2008; 48: 486-498.

[13] Sezer M, Yalcinbas S, Sahin N. Approximate solution of multi-pantograph equation with variable coefficients. *Journal of Computational and Applied Mathematics*. 2008; 214: 406-416.

[14] Li D, Liu MZ. Runge-Kutta methods for the multi-pantograph delay equation. *Applied Mathematics and Computation*. 2005; 163: 383-395.

[15] Alomari AK, Noorani MSM, Nazar R. Solution of delay differential equation by means of homotopy analysis method. *Acta of Applied Mathematics*. 2009; 108: 395-412.
[16] Yu ZH. Variational iteration method for solving the multi-pantograph delay equation. *Physics Letters A*. 2008; 372: 6475-6479.
[17] Saadatmandi A, Dehghan M. Variational iteration method for solving a generalized pantograph equation. *Computers and Mathematics with Applications*. 2009; 58: 2190-2196.
[18] Yüzbaşı S. Laguerre approach for solving pantograph-type Volterra integro-differential equations. *Applied Mathematics and Computation*. 2014; 232: 1183-1199.
[19] Yalinbas S, Aynigul M. A collocation method using Hermite polynomials for approximate solution of pantograph equations. *Journal of the Franklin Institute*. 2011; 348: 1128-1139.
[20] Tohidi E, Bhrawy AH, Erfani K. A collocation method based on Bernoulli operational matrix for numerical solution of generalized pantograph equation. *Applied Mathematical Modelling*. 2013; 37(6): 4283-4294.
[21] Ansari KJ, Özger F. Pointwise and weighted estimates for Bernstein-Kantorovich type operators including beta function. *Indian Journal of Pure and Applied Mathematics*. 2024; 13: 1-13.
[22] Savaş E, Mursaleen M. Bézier type Kantorovich q-Baskakov operators via wavelets and some approximation properties. *Bulletin of the Iranian Mathematical Society*. 2023; 49: 68.
[23] Özger F, Aslan R, Ersoy M. Some approximation results on a class of Szász-Mirakjan-Kantorovich operators including nonnegative parameter α. *Numerical Functional Analysis and Optimization*. 2025; 46: 481-484.
[24] Tremblay R, Gaboury S, Fugère BJ. A new class of generalized Apostol-Bernoulli polynomials and some analogues of the Srivastava-Pintér addition theorem. *Applied Mathematics Letters*. 2011; 24: 1888-1893.
[25] Agoh T, Dilcher K. Integrals of products of Bernoulli polynomials. *Journal of Mathematical Analysis and Applications*. 2011; 381: 10-16.
[26] Edwards R, Leeming DJ. The exact number of real roots of the Bernoulli polynomials. *Journal of Approximation Theory*. 2012; 164: 754-775.
[27] El-Desouky BS, Gomaa RS. A new unified family of generalized Apostol-Euler, Bernoulli and Genocchi polynomials. *Applied Mathematics and Computation*. 2014; 247: 695-702.
[28] Choi J, Kim YH. A note on high order Bernoulli numbers and polynomials using differential equations. *Applied Mathematics and Computation*. 2014; 249: 480-486.
[29] Feng L, Wang W. An algorithm for computing mixed sums of products of Bernoulli polynomials and Euler polynomials. *Journal of Symbolic Computation*. 2015; 66: 84-97.
[30] Kim DS, Kim T, Dolgy DV. A note on degenerate Bernoulli numbers and polynomials associated with p-adic invariant integral on $\mathbb{Z}_p$. *Applied Mathematics and Computation*. 2015; 259: 198-204.
[31] Kim TK. Barnes' type multiple degenerate Bernoulli and Euler polynomials. *Applied Mathematics and Computation*. 2015; 258: 556-564.
[32] Ordokhani P, Ordokhani Y, Babolian E. Numerical solution of fractional pantograph differential equations by using generalized fractional-order Bernoulli wavelet. *Journal of Computational and Applied Mathematics*. 2017; 309: 493-510.
[33] Lehmer DH. A new approach to Bernoulli polynomials. *The American Mathematical Monthly*. 1998; 95: 905-911.
[34] Mashayekhi S, Ordokhani Y, Razzaghi M. Hybrid functions approach for nonlinear constrained optimal control problems. *Communications in Nonlinear Science and Numerical Simulation*. 2012; 17: 1831-1843.
[35] Sahin N, Yüzbaşı S, Gülşü M. A collocation approach for solving systems of linear Volterra integral equations with variable coefficients. *Computers and Mathematics with Applications*. 2011; 62: 755-769.
[36] Yüzbaşı S, Sahin N, Sezer M. A collocation approach to solving the model of pollution for a system of lakes. *Mathematics and Computational Modeling*. 2012; 55: 330-341.
[37] Yüzbaşı S. A numerical approach for solving the high-order linear singular differential-difference equations. *Computers and Mathematics with Applications*. 2011; 62: 2289-2303.
[38] Yüzbaşı S. A numerical approximation for Volterra's population growth model with fractional order. *Applied Mathematics and Modeling*. 2013; 37: 3216-3227.
[39] Yüzbaşı S. Bessel collocation approach for solving continuous population models for single and interacting species. *Applied Mathematics and Modeling*. 2012; 36: 3787-3802.
[40] Yüzbaşı S, Sahin N, Sezer M. Bessel polynomial solutions of high-order linear Volterra integro-differential equations. *Applied Mathematics and Modeling*. 2011; 62: 1940-1956.

[41] Yüzbaşı S, Sahin N, Sezer M. Numerical solutions of systems of linear Fredholm integro-differential equations with Bessel polynomial bases. *Computers and Mathematics with Applications*. 2011; 61: 3079-3096.
[42] Kreyszig E. *Introductory Functional Analysis with Applications*. India: Wiley India Pvt. Ltd.; 2007.
[43] Behroozifar M, Habib N. A numerical approach for solving a class of fractional optimal control problems via operational matrix Bernoulli polynomials. *Journal of Vibration and Control*. 2017; 24(12): 2494-2511. Available from: https://doi.org/10.1177/1077546316688608.
[44] Horvat V. On polynomial spline collocation methods for neutral Volterra integro-differential equations with delay arguments. In: *Proceedings of the 1st Conference on Applied Mathematics and Computation*. Dubrovnik, Croatia; 1999. p.113-128.
[45] Bellour A, Bousselsal M. Numerical solution of delay integro-differential equations by using Taylor collocation method. *Mathematical Methods in the Applied Sciences*. 2014; 37: 1491-1506.
[46] Behera S, Ray SS. An efficient numerical method based on Euler wavelets for solving fractional order pantograph Volterra delay-integro-differential equations. *Journal of Computational and Applied Mathematics*. 2022; 406: 113825.
[47] Gülşü M, Sezer M. A collocation approach for the numerical solution of certain linear retarded and advanced integrodifferential equations with linear functional arguments. *Numerical Methods for Partial Differential Equations*. 2011; 27: 447-459.